PNC TG033 82-01(5)

Thermal and Hydraulic Experiments of JOYO Fuel Subassembly

K. Miyaguchi*, K. Satoh** and T. Iguchi**

* Experimental Fast Reactor Division
** Sodium Engineering Division
Oarai Engineering Center

January 1982

This document is prepared for the Third Japan/USSR Seminar on Methods of Testing of Equipment, Structural Materials and Fuel of JOYO, BOR-60 and BR-10, Tokyo, Japan, February 15-18, 1982.

POWER REACTOR AND NUCLEAR FUEL DEVELOPMENT CORPORATION

PNC TG033 82-01 (5)
Jan, 1982

Thermal and Hydraulic Experiments of JOYO Fuel Subassembly

K. Miyaguchi*, K. Satch** and T. Iguchi**

* Experimental Fast Reactor Division

** Sodium Engineering Division

Abstract

Several series of thermal and hydraulic experiments have been conducted using full mock-ups of JOYO fuel subassemblies.

This paper describes the test results of cross-flow mixing and pressure loss in wire-wrapped pin bundles.

It also presents the comparison between cross-flow mixing experiments and calculations by SWIRL code.

I. Introduction

The design of a fast reactor fuel subassembly requires accurate prediction of thermal-hydraulic characteristics to ensure safety and economy, because it consists of a compactly assembled fuel pins with high power density. Hence hydraulic characteristics were investigated using water, and endurance tests were conducted in flowing sodium. Cross-flow mixing in wire-wrapped pin bundles was studied both in water flow and sodium flow experiments.

The thermal and hydraulic experiments conducted for JOYO MK-I and MK-II subassemblies are summarized as follows:

For the MK-I subassembly ;

- Pressure Loss Characteristics in Pin Bundles
- Pressure Loss Characteristics at Inlet Nozzle including Flow Orifices
- Velocity Distribution right behind Pin Bundle
- Flow-Induced Vibration of Subassembly
- Cross-Flow Mixing in Pin Bundle
- Endurance Tests in Flowing Sodium
- Flow-Induced Vibration of Distorted Pin Bundles (in Progress)

For the MK-II subasembly ;

- Pressure Loss Characteristics in Pin Bundle
- Pressure Loss Characteristics at Inlet Nozzle including Orifices
- Leak flow at the Spherical Seat
- Endurance Tests in Flowing Sodium
- Pressure Loss and Flow Distribution Characteristics for irradiaton Test Assemblies

All experiments are already finished except those for distorted pin bundles.

From the above experiments, two experiments were selected and presented here, that is, the cross-flow mixing experiments for MK-I subassemblies and the pressure loss characteristics for MK-II subassemblies.

II. Cross-Flow Mixing in Wire-Wrapped Pin Bundles

Cross-flow mixing coefficients for JOYO core and blanket subassemblies were obtained by analyzing temperature distributions measured in the simulation experiments. Full mock-ups of the JOYO core and blanket subassemblies were used in a sodium loop, since the effects of pin bundle geometry on the mixing coefficient were not clear. Power distributions, however, were not simulated. Only several pins were electrically heated at constant linear heat rate. Specifications of mock-ups are shown in Table 2.1. Sodium temperature distributions in simulated pin bundels were measured for different power distributions and different sodium flow rates, using 0.65 mm O.D. C-A thermocouples fitted on dummy pins. Fig. 2.1 shows the outlines of heater pins together with the elevations at which temperature profiles were measured. Test sections were covered with thermal insulator over which guard heaters were wound.

In parallel with the experiments, an analytical code, SWIRL was developed which considered periodic swirling flows along spiral wire spacers. The mixing coefficients were determined so that the calculated temperature distributions using those coefficients might be best fitted to the measured temperature distributions in the mock-up subassemblies. The mathematical model of the SWIRL code is summarized as follows:

i) A subchannel analysis method is employed.

ii) Finite-difference equation for steady mass and energy balances are solved as an initial value problem.

iii) Forced cross-flows along wrapping wires, w_{ij}, are presented by the following expressions:

$$w_{ij} = \begin{cases} C_s(\gamma U)^* d_s \dfrac{\pi do}{s} \cos\Psi & \text{(for inner subchannels)} \quad (2.1) \\ C_s(\gamma U)^* d_s \dfrac{\pi do}{s} \cdot \dfrac{1+\cos\Psi}{2} & \text{(for peripheral subchannels)} \quad (2.2) \end{cases}$$

$$(\gamma U)^* = \begin{cases} \gamma_i U_i & (\text{for } w_{ij} > 0) \\ \gamma_j U_j & (\text{for } w_{ij} < 0) \end{cases}$$

Where C_s is an unknown parameter determined by experimental data, γ the specific weight of coolant, U_i the bulk velocity in the subchannel i, ds the diameter of wrapping wire, ℓs the wire-wrapping pitch, do the pin outer diameter and Ψ the phase angle of the spiral wire.

The flow sweep, that is, forced cross-flow due to spiral wires takes an important part in the cross-flow mixing for wire-wrapped pin bundles. In the present studies w_{ij} represents the flow sweep where C_s should be determined by comparisons between measured and calculated temperature distributions. For comparing with other investigators' data, w_{ij} is rewritten in a more general form like β value used in the COBRA-II code,[2] where β represents the averaged mixing rate per unit axial length normalized by the subchannel flow rate. Similar mixing rates for the present cases are obtained by following procedures:

The increment of axial distance, z is ℓs while the phase angle of a spiral wire gains 2π, hence the following relation is obtained.

$$\frac{dz}{d\Psi} = \frac{\ell s}{2\pi} \quad (2.3)$$

Substituting Eq. (2.3) into Eq. (2.1), the cross-flow rate in the interval z, z+dz is given as follows:

$$w_{ij}dz = C_s(\gamma U)^* \frac{ds\, do}{2} \cos\Psi \, d\Psi \quad (2.4)$$

It is assumed in the SWIRL code that the flow sweep is caused in the interval $[-\pi/2, \pi/2]$, therefore, the total crocss-flow from subchannel i to j over one wire-wrapping pitch, W_{ij}, is given by the following equation.

$$W_{ij} = C_s \frac{\gamma\, ds\, do}{2} \int_{-\pi/2}^{\pi/2} U_i \,\mathrm{Cos}\Psi\, d\Psi \qquad (2.5)$$

The axial velocity, U_i is nearly constant along the axial direction, therefore the mean value, U_i is substituted for $\bar{U}_i$ in Eq. (2.5) and taken out of the integral sign. Consequently, the following relation is obtained.

$$W_{ij} = C_s \,\gamma\, \bar{U}_i \, d_s \, d_0 \qquad (2.6)$$

Hence, the average mixing rate per unit axial length, $\bar{W}_{ij}$, is given by

$$\tilde{W}_{ij} = \frac{C_s \,\gamma\, \bar{U}_i \, d_s \, d_o}{\ell_s} \qquad (2.7)$$

and in a normalized form similar to β,

$$\beta = \frac{\bar{W}_{ij}/d_s}{\gamma\, \bar{U}_i}$$

, that is,

$$\beta = C_s \frac{d_0}{\ell_s} \qquad (2.8)$$

is obtained.

The normalized mixing rate, β seems to be inversely proportional to the slope of wrapping wires, as indicated in the experiments by Baumann and Hoffman[1]. Consequently a following new parameter

$$\kappa = \beta \times \frac{\ell s}{p} \qquad (2.9)$$

seems to be nearly constant for any wire-wrapped pin bundles. Therefore we had bettrer evaluate κ rather than β to compare different experimental data of wire-wrapped pin bundles.

Experimental results for the JOYO radial blanket mock-up are shown in Fig.2.2 (a) and (b) in the form of normalized temperature rise versus shbchannel number. Calculated temperature rises by SWIRL code are plotted together. In the case of Fig. 2.2(a) six heater pins were simultaneously heated. Measured temperature profiles at the elevations 3-3' and 4-4' agree well with the calculated results by SWIRL code. Only in subchannel no. 10 and 21 at the elevation 3-3' discrepancies between the experiment and the calculation are found because of steep temperature gradient in their neighborhoods.

Fig. 2.2(b) represents a case in which only one heater pin, H4 was heated. The aim of this experiment was to investigate the effect of swirling flow around a pin bundle and to confirm the flow sweep rate in peripheral subchannels. Calculated results are in good agreement with experimental data in this case, too. In above two cases Cs was chosen to be 0.7 for inner subchannels, 2.0 for peripheral subchannels and 0.35 for bundaries between inner subchannels and peripheral ones. Good agreements between calculations and experiments were obtained using the identical set of Cs values as well for other temperature profiles at about the same flow rate, not cited in the present paper. This fact indicates that the set of Cs values decided from the present experiment can be applied to predict temperature profiles for any power distribution in a subassembly of the same geometry as the present mock-up.

Similar experiments for the JOYO core subassembly and the analysis by SWIRL code were performed.

Seven symmetrically arranged heater pins were simultaneously heated. Three symmetrical temperature profiles in diagonal direction and in peripheral subchannels are compared in Fig. 2-3(a) and (b), respectively. The three profiles in each figure are not strictly symmetric because of the asymmetry of the phase angle of wrapping wire. SWIRL calculations clearly show the asymmetry and agree well with experimental data in both figures. In Fig. 2.3(a) Cs was chosen to be 0.6 for inner subchannels, 2.0 for peripheral subchannels and 0.3 for the boundary between inner subchannels and peripheral ones. In Fig. 2.3(b), however, best fitted values of Cs for each region were 0.5, 2.0 and 0.25, respectively. Hence it seems that the best fitted values of Cs are slightly dependent on Reynolds number.

The Cs values for inner region decided from the present experiments are summerized in Table 2.2. Corresponding κ values are 0.59 for the blanket subassembly and 0.55 for the core one, respectively. The comparison between κ values for our data and for other investigators' data is shown in Table 2.3. As expected, the table shows a nearly constant κ value of about 0.6 for different wire-wrapped pin bundles.

It is concluded from the present study and the comparison with other investigators' data that the dimensionless mixing rate, κ is nearly constant for wire-wrapped pin bundles of different p/d and different ls/d and that SWIRL code can predict temperature distributions in any pin bundle spaced by wrapping wires.

III. Pressure Loss Characteristics in Wire-Wrapped Pin Bundles

Pressure loss characteristics were investigated on the effects of pin pich-to-diameter ratio, wire wrap lead-to-pin diameter ratio and Reynolds number. Rehme[6] and Novendstern[7] investigated earlier such effects and reported semi-empirical equations for the friction factor in a wire-wrapped pin bundle. Markley[8] obtained the pressure loss characteristics in laminar flow range for different p/d and ls/d. Their correlations, however, proved to be somewhat unsatisfactory when applied to our experimental data. New correlations were therefore obtained which are in better agreement with our data.

Five full mock-ups of JOYO MK-II fuel subassembly were tested in the water loop. Their bundle specifications are the same except wire wrap lead, as shown in Table 3.1. In Fig. 3.1 the experimental data are plotted together with the data for Monju subassembly mock-ups in the form of modified friction factor, f_N versus modified Reynolds number, Re_N. f_N and Re_N are defined almost similarly to Novendstern's equation as follows:

$$f_N = \left(\Delta P \cdot \frac{De}{L} \right) / \left(\frac{\gamma V^2}{2g} \cdot M \cdot X_N{}^2 \cdot \left(\frac{De}{De_l}\right)^{1.5} \right) \tag{3.1}$$

$$Re_N = Re_N \cdot X_N \cdot \frac{De_l}{De} \tag{3.2}$$

$$M = \left\{ \frac{1.034}{(p/d)^{0.124}} + \frac{29.7(p/d)^{6.94} Re^{0.086}}{(\rho s/d)^{2.239}} \right\}^{0.885} \tag{3.3}$$

$$X_N = \frac{\sum_{i=1}^{3} ni\ Ai}{\sum_{i=1}^{3} ni\ Ai \left(\frac{De_i}{De_l}\right)^{0.714}} \tag{3.4}$$

where

- P : Pressure drop through the axial length L
- Re : bundle mean Reynolds number
- γ : specific weight of water
- V : bundle mean velocity
- d : pin diameter
- p : pin pitch
- De : bundle mean hydraulic diameter
- Dei : hydraulic diameter of i-th region subchannel
- Ai : free flow area of i-th region subchannel
- ni : number of i-th region subchannel
- suffix 1 : inner region
- suffix 2 : peripheral region
- suffix 3 : corner region

The experimental data indicate that the flow pattern in a pin bundle changes at Reynolds number of about 8000. Hence the Reynolds number range for the present data is divided into two parts, that is, higher Reynolds number range and lower one. For each range the best fitted correlation for f_N was obtained as follows:

$$f_N = \frac{47.4}{Re_N} + \frac{0.074}{Re_N^{0.118}} \qquad \text{for } 1.3 \times 10^3 < Re_N < 1 \times 10^4 \qquad (3.5)$$

$$f_N = 0.237\, Re_N^{-0.226} \qquad \text{for } 1 \times 10^4 < Re_N < 7 \times 10^4 \qquad (3.6)$$

Fig. 3.2 shows the pressure loss characteristics of a wire-wrapped pin bundle over wide Reynolds number range including laminar flow regime. This figure indicates a smooth transition of the friction factor when the Reynolds number varies from laminar range to turbulent one, as reported in the paper by Markley[8)]. It seems that the smooth transition results from staggered pin arrangement and cross-flows due to wrapping wires. A smooth friction factor curve for flows across staggered pin arrangement was earlier found by Burgelin, Brown and Doberstein[9)]. It is concluded from the present investigation that the friction factor for wire-wrapped pin bundles of staggered arrangement has a smooth transition characteristic and that experimental data should be correlated with three different equations for liminar, transition and turbrulent flow regime, respectively.

IV. Summary

Cross-flow mixing and pressure loss characteristics over wide Reynolds number range were experimentally investigated and discussed in some detail. These two characteristics are peculiar to pin bundles with spiral spacers and the most important for the thermal hydraulic design of a subassembly with such spacers. From the present studies following conclusions were obtained :

1) The dimensionless mixing rate, κ is neary constant for any wire-wrapped pin bundle.
2) The friction factor for a wire-wrapped pin bundle of staggered arrangement has a smooth transition characteristic.

V. Acknowledgement

The authors are indebted to Dr. K. Takahashi, to Mr. T. Suzuki and to Mr. S. Sasaki for the mixing experiments and to Mr. T. Kogawa for the flow characteristic experiments of MK-II subassemblies. Their contributions are gratefully acknowledged.

References

1) Koyama T., Horikawa T. et al., "Development of an Analytical Code for Inter-Subchannel Sodium Mixing in LMFBR Subassemblies", PNC Report

2) Rowe D.S., "Cross-Flow Mixing Between Parallel Flow Channels During Boiling" (Part 1), "COBRA-Computer Program for Coolant Boiling in Rod Arrays", BNWL-371 Pt. 1, March 1967

3) Baumann W., Hoffmann H., "Coolant Cross-Mixing of Sodium Flowing in Line through Multi-Rod Bundles with Different Spacer Arrangements", Trogia, 1971

4) Okamoto Y., Akino A., JAERI-momo 4577

5) Todreas N.E., Turi J.A., "Interchannel Mixing Rates in Wire-Wrapped Liquid Metal Fast Breeder Reactor Fuel Assemblies", Trans. ANS (1972)

6) Rehme K., "Pressure Drop Correlations for Fuel Element Spacers", Nuclear Technology Vol. 17 January (1973)

7) Novendstern E.H., "Turbulent Flow Pressure Drop Model for Fuel Rod Assemblies Utilizing a Helical Wire-Wrap Spacer System", Nuclear Engineering and Design 22 (1972) 19-27

8) Markley R.A. and Engel F.C., "LMFBR Blanket Assembly Heat Transfer and Hydraulic Test Data Evaluation", IAEA/IWGFR Specialists' Meeting on FBR S/A under Nominal and Nonnominal Operating Conditions, Feb., 1979

9) Bergelin O.A., G. A. Brown and S.C. Doberstein, Trans. ASME, 74:53 (1952)

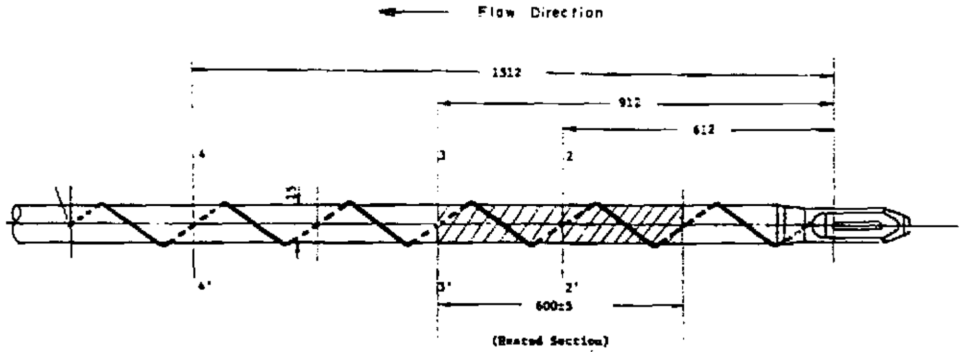

Elevations of Temperature Measurement for JOYO Blanket Mock-up Subassembly

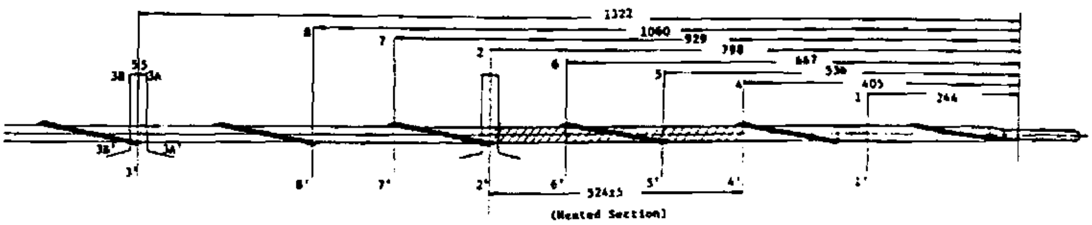

Elevations of Temperature Measurement for JOYO Core Mock-up Subassembly

Fig. 2.1 Elevations where Temperature Distributions were measured for JOYO Core and Blanket Mock-up Subassemblies

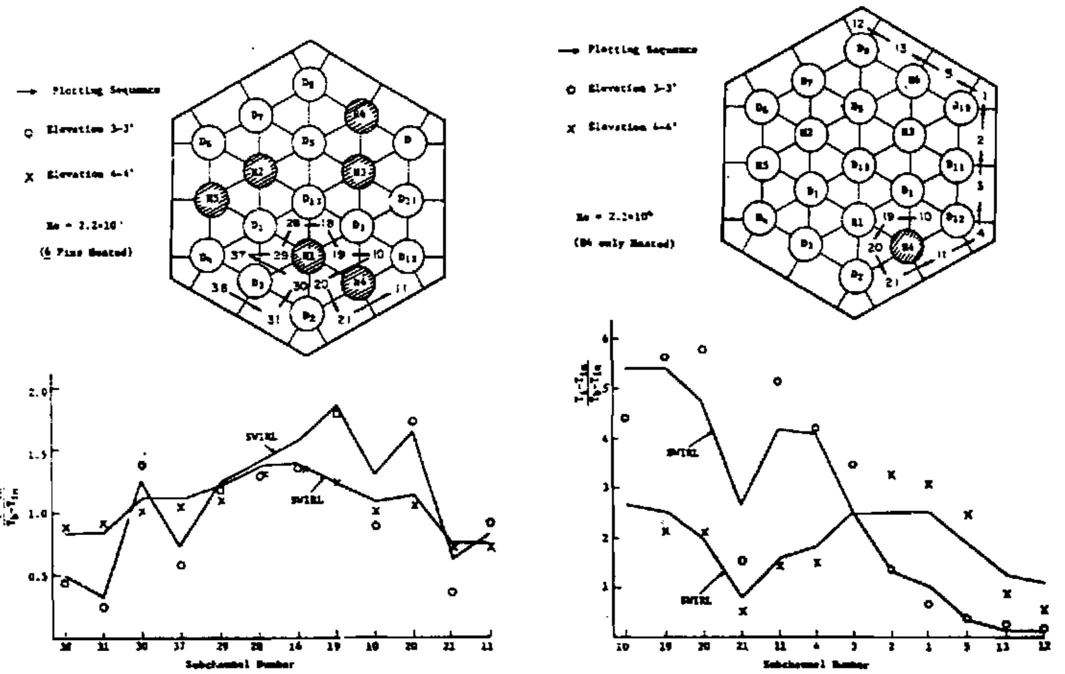

Fig. 2.2(a) Temperature Profiles when 6 Pins are heated

Fig. 2.2(b) Temperature Distribution along Prepherical Subchannels

Fig. 2.2 Measured and Calculated Temperature Profiles in a 19-Pin Wire-Wrapped Bundle Simulating JOYO Blanket Subassembly

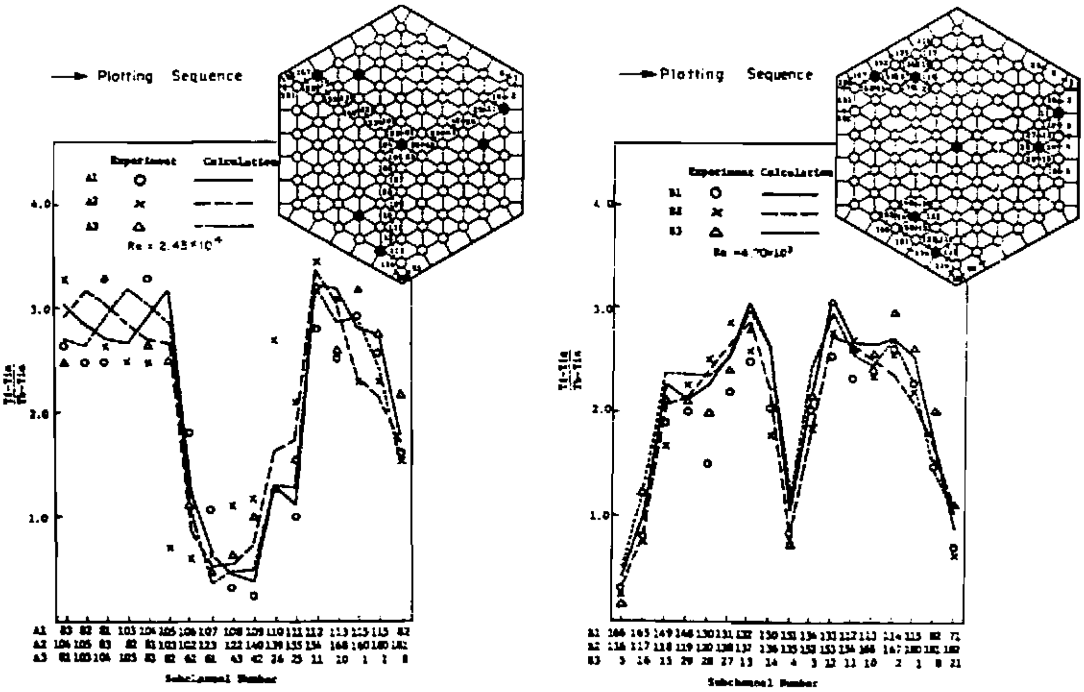

(a) Radial Temperature Profiles at the Elevation 2-2'

(b) Peripheral Temperature Profiles at the Elevation 2-2'

Fig. 2.3 Measured and Calculated Temperature Profiles in a 91-Pin Wire-Wrapped Bundle Simulating JOYO Core Subassembly

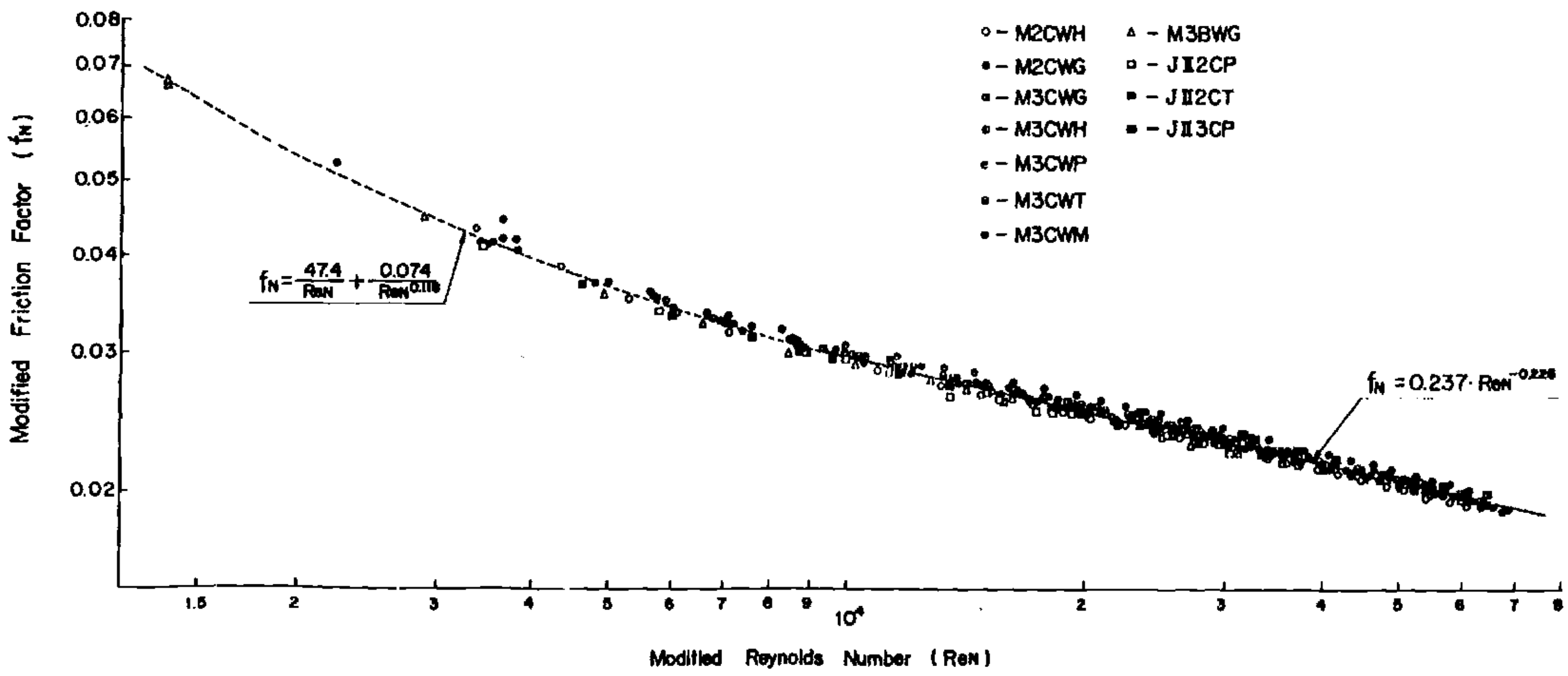

Fig. 3.1 Relations of Modified Friction Factor vs. Modified Reynolds Number

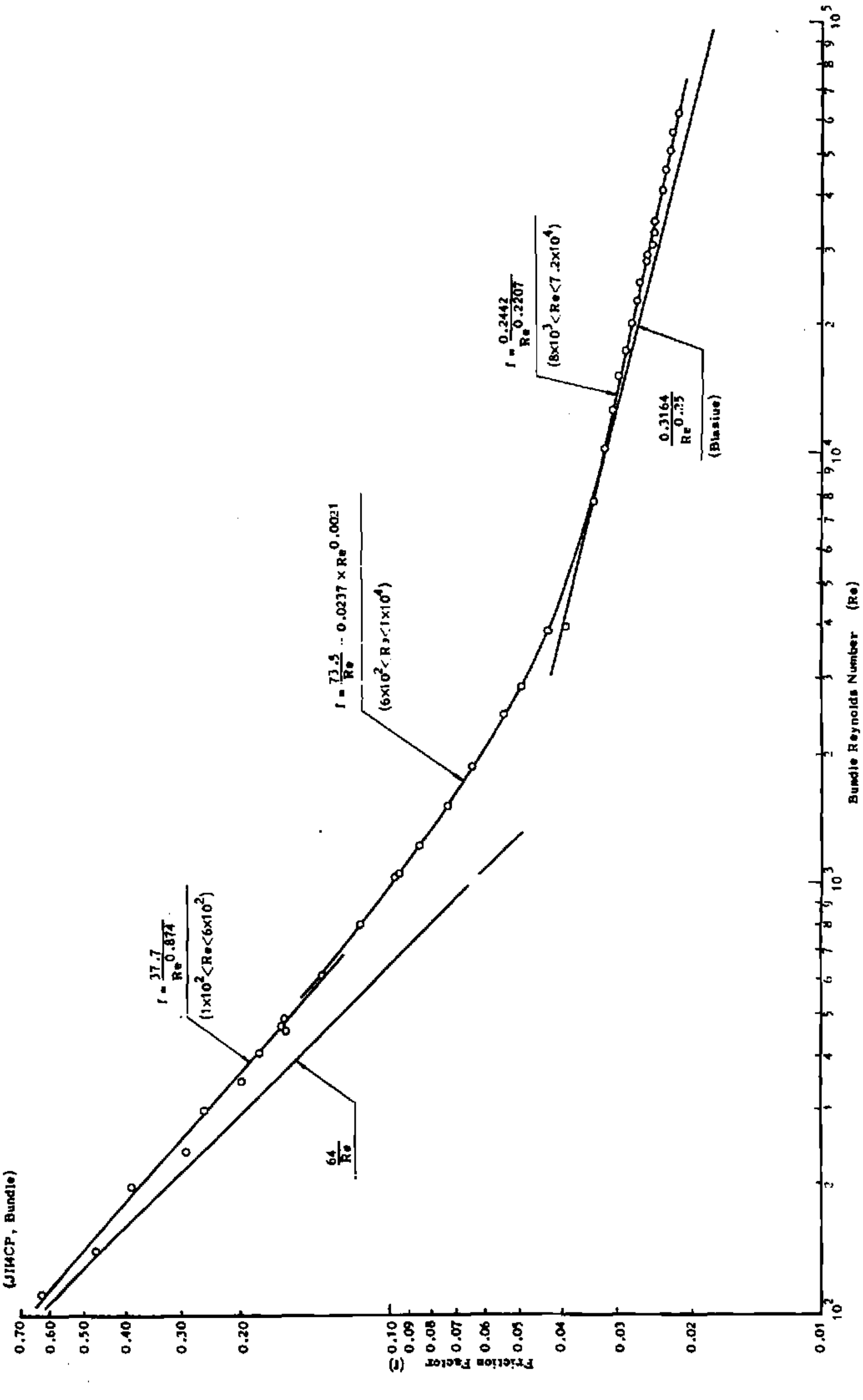

Fig. 3.2 Friction Factor of Fuel Pin Bundle as a Function of Bundle Reynolds Number

Table 2.1 Specifications of Mock-up Subassemblies for Cross-Flow Mixing Experiments

	Number of Pins	Pin Diameter d_p (mm)	Pin Pitch P (mm)	Wire Lead ℓ_s (mm)	Wire Diameter d_w (mm)	Number of Heater Pins	Heated Length (mm)	Flat to Flat Distance of Wrapper Tube
JOYO (Blanket)	19	15.0	16.42	300	1.3	6	600	74.6
JOYO (Core)	91	6.3	7.60	262	1.2	7	524	74.6

Table 2.2 C_s Values for JOYO and MONJU Subassemblies

	p/d_p	ℓ_s/d_p	ℓ_s/p	C_s	Reynolds Number
JOYO (Blanket)	1.095	20.0	18.3	0.6~0.7	3000~22000
JOYO (Core)	1.206	41.6	34.5	0.5~0.7	5000~65000

Table 2.3 Comparisons of κ Values for Wire-Wrapped Pin Bundles with Different p/d and ℓ_s/p

	Number of Pins	p/d	ℓ_s/p	Reynolds No. $\times 10^{-4}$	κ	Reference
PNC (JOYO Blanket)	19	1.09	18.3	0.3~2.3	0.59	
PNC (JOYO Core)	91	1.21	34.5	0.5~6.5	0.55	
PNC (MONJU Core)	169	1.21	38.9	0.5~5.5	0.62	
JAERI (No.1)	91	1.21	34.5		0.60	4)
GFK (by Hoffmann)	61	1.32	38.0	1~5	0.66	3)
GFK (by Baumann & Möller)	61	1.167	14.3	2~3	0.57~0.76	5)
JAERI (No.2)	91	1.22	33.3	0.4~1.5	0.77~0.87	5)
Millholen & Sutey	37	1.25	42.3	4.1	0.51	5)
SKOK (No.1)	7	1.355	19.6	4.2	0.40	5)
SKOK (No.2)	7	1.142	12.5	2.5~5.5	0.50~1.0	5)
SKOK (No.3)	7	1.142	18.1	4.2	0.54	5)
SKOK (No.4)	7	1.142	25.0	4.2	0.75	5)
SKOK (No.5)	7	1.065	18.7	4.2	0.37~0.56	5)

Table 3.1 Specifications of Joyo MK-II Subassembly Mock-ups

	Number of Pins	Pin Diameter d (mm)	Pin Pitch p (mm)	Wire Lead ℓs (mm)	Wire Diameter (mm)	ℓs/d
JII1CT	127	5.5	6.47	292	0.9	53.0
JII2CP	127	5.5	6.47	293	0.9	53.3
JII2CT	127	5.5	6.47	211	0.9	38.4
JII3CP	127	5.5	6.47	211	0.9	38.4
JII4CP	127	5.5	6.47	209	0.9	38.0